

# Analysis of Drone Propagation With Ray Tracing From Sub-6 GHz Upto Terahertz Frequencies in a Real World Urban Environment

Muhammad Usman Sheikh, Kalle Ruttik, Norshaida Saba, Edward Mutafulungwa, Riku Jäntti, and Jyri Hämäläinen  
Department of Communications and Networking, Aalto University, 02150 Espoo, Finland  
Email: {muhammad.sheikh, kalle.ruttik, norshahida.saba, edward.mutafulungwa, riku.jantti, jyri.hamalainen}@aalto.fi

**Abstract**—Unmanned aerial communication platforms have been recently considered as an effective solution to provide homogeneous and extended network coverage to terrestrial users. Unmanned Aerial Vehicles (UAVs) are expected to increase the network reliability and users' Quality of Experience (QoE). The first target of this paper is to analyze the propagation characteristics of drone transmission at different frequencies i.e., 3.5 GHz, 28 GHz, 60 GHz, and up to 180 GHz with 20 GHz step. In the considered setup drone is flying at different heights i.e., from 50m up to 250m altitude and we carry out 3D ray tracing simulations assuming a propagation environment that is defined by the real building data from Helsinki city. Ground users are placed outdoors. We study the validity of a previously proposed geometrical Line of Sight (LOS) probability model between ground user and drone, and based on simulations we propose new modeling parameters. In the second part of the paper, the ray tracing results are compared with the analytical reference model. Finally, a new set of parameters is proposed for tuned analytical model based on acquired ray tracing results. The proposed analytical model provides significantly low Root Mean Square Error (RMSE) when compared with the analytical reference model.

**Index Terms**—Drone propagation, unmanned aerial vehicle, ray tracing, millimeter wave, simulations.

## I. INTRODUCTION

In a traditional cellular network, the communication between the Transmitter (Tx) and the Receiver (Rx) is mainly established by using a fixed infrastructure i.e., fixed Base stations (BSs) [1]. In order to temporarily increase the area capacity of a cellular network the state-of-art solution is to use a mobile cell. Mobile cell sites are transportable infrastructures on trucks or trailers (also known as, cell-on-wheels), allowing fast installation in restricted spaces. They are useful in coping with the problem of sudden increase of mobile traffic in case of extraordinary events such as trade fairs, sports events, and concerts [2], [3]. They are also used as a replacement of the conventional network infrastructure in case of catastrophes and critical situations like earthquakes, cyclones, tsunamis, fire and floods. Recently new class of flying cell has emerged based on Unmanned Aerial Vehicles (UAVs), commonly referred to as drones, and Low-Altitude Aerial Platforms (LAPs) i.e., balloons as a feasible solution for wireless network recovery [4], [5]. The benefits of using UAVs over conventional cell-on-wheels includes lower cost, smaller size, and quicker deployment. The drawback of UAV cell is much smaller operation

time compared with cell on wheel due to the energy storage constraints of the flying drones.

There are several deployment options for a drone-based cell:

- 1) Base station (BS) on drone: Small cell base station is mounted on a drone and connected to the core network via some wireless backhaul link [4].
- 2) Remote radio head (RRH) on drone: Base station is kept on the ground, but digital IQ of the data is send over a wireless front-haul link to the RRH mounted on the drone.
- 3) Radio relay (RR) on drone: Base station is kept on the ground, but analog RF signal is send over a wireless front-haul link to the RRH mounted on a drone [5].

Wireless communication systems operating at sub-6 GHz frequency bands are no longer sufficient to support the huge data rate and network capacity demand of the future. The recent advancement in transceiver and e.g. photonic technologies have made Millimeter Wave (mmWave) and Terahertz (THz) frequency bands attractive for the industry and academia [6] since large chunks of frequency bands are available at mmWave and THz frequencies and can be utilized to acquire significantly high data rates. High carrier frequencies are also well applicable for fixed high speed backhaul links. While the small wavelength at higher frequencies facilitates the integration of large number of antenna elements, the use of directive antenna arrays at the transmitter and receiver becomes feasible [7]. Yet, there are challenges as well: Path loss can be heavy at high carrier frequencies, and for certain frequency bands there is also high atmospheric absorption loss as explained in [7].

In order to plan and design an efficient communication network operating at mmWave and THz frequency bands, accurate radio channel characterization and coverage prediction methodology are required. The deterministic Ray Tracing (RT) approach becomes highly valuable since it is able to efficiently characterize the propagation in various environments [8], [9]. By default, the UAV communication experiences different propagation environment compared with the terrestrial communication [10], and therefore the conventional path loss, LOS probability, and fading models of terrestrial communication can't be directly applied for the drone communication. Ac-

cordingly, several studies have proposed the UAV altitude and an elevation angle dependent models for the drone communication [2], [11]. Since the UAV can freely move around and fly at different heights, the authors of [12] discussed about the optimal 3D placement of the drone satisfying the SINR requirements of terrestrial UEs. Furthermore, authors of [13] carried out the coverage, capacity and interference analysis of UAV base station using 3D ray tracing, while assuming uniformly distributed buildings that follow the Rayleigh distribution for building height. Our objective is to further expand the understanding of the drone based communication by analyzing the characteristics of signal propagation when utilizing real building data of urban city (Helsinki). Drone transmission is carried out at different heights i.e., from 50m up to 250m at different frequencies of operation i.e., from 3.5 GHz to 180 GHz. In addition, we propose an analytical LOS probability and path loss model which gives minimum RMSE with respect to the ray tracing simulation results.

The rest of the paper is organized as follows. Section II describes the analytical model for the drone propagation. Section III gives details about the simulation tool, parameters and simulation setup. Section IV provides a discussion on the simulation results, and finally Section V concludes the paper.

## II. ANALYTICAL MODEL FOR UAV PROPAGATION

Let us consider the propagation model introduced in [11]. The Line of Sight (LOS) probability for a link between a UAV and the terrestrial UE is approximated by Eq 1,

$$\text{PR}_{LOS}(\theta) \approx \frac{1}{1 + a \exp(-b(\theta - a))} \quad (1)$$

$$\text{PR}_{NLOS}(\theta) = 1 - \text{PR}_{LOS}(\theta) \quad (2)$$

where parameters  $a$  and  $b$  are environment dependent,  $\theta = \arctan\left(\frac{h_D - h_U}{r}\right)$  is the elevation angle in degrees, from UE towards the drone,  $h_D$  and  $h_U$  are the heights of the drone and a terrestrial UE above the ground, respectively, and  $r$  is the ground distance between the drone and the terrestrial UE. In a typical urban area, we have  $a = 9.61$  and  $b = 0.16$  [14]. The mean path loss in dB scale is given as:

$$L = 20 \log_{10} \left( 4\pi \frac{d}{\lambda} \right) + \text{PR}_{LOS} \eta_{LOS} + (1 - \text{PR}_{LOS}) \eta_{NLOS} \quad (3)$$

where  $\lambda$  denotes the wavelength,  $d = \sqrt{(h_D - h_U)^2 + r^2}$  is the total link distance and  $\eta_{LOS}$  and  $\eta_{NLOS}$  are the average additional losses due to obstacles in LOS and non-line-of-sight (NLOS) conditions, respectively. In urban case, we have  $\eta_{LOS} = 1$  dB and  $\eta_{NLOS} = 20$  dB.

## III. SIMULATION METHODOLOGY

We have carried out a campaign of 3D ray tracing simulations using a MATLAB based tool developed by the authors of this paper. The Image Theory (IT) method is used for finding the propagation paths with reflections and diffractions. While our aim was to compare the ray tracing simulation results with results obtained from the analytical model, we

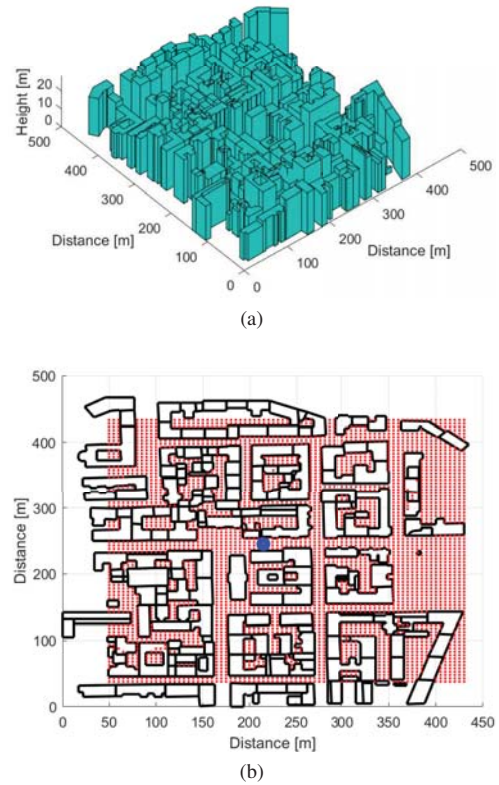


Fig. 1. Area under consideration, (a) 3D view of buildings, and (b) 2D view with user distribution.

carried out extensive numerical simulations. In the considered practical scenario a single drone is at a static position above rooftops to provide an emergency coverage in given urban area. For simulations, we have used a real building data of Helsinki city downtown area. Fig. 1(a) illustrates the three-dimensional building data of the area that is considered for this research work. There are buildings of irregular shapes with different heights and types, whereas the maximum height of the buildings is 28m. The widths of the roads and streets vary. The two dimensional map (top view) of the considered area is illustrated in Fig. 1(b). The grid of red dots in Fig. 1(b) shows the positions of the terrestrial outdoor users with 5m mutual separation at the ground level, whereas the blue mark in the middle represents the ground projection of the UAV position. All the receiver locations are considered at 1.5 m height. An omni directional antenna is assumed at both the user and UAV end. We have mainly focused on the downlink performance, and the maximum transmission power in the downlink direction is set to 30 dBm (1 watt). It is assumed that the transmitter operates with maximum allowed power without any power control.

## IV. SIMULATION RESULTS AND DISCUSSION

First we analyze the ray tracing simulation data which we have acquired by using a Helsinki city downtown building information and a grid of user locations as shown in Fig. 1(b), and compute the percentage of the outdoor users in LOS

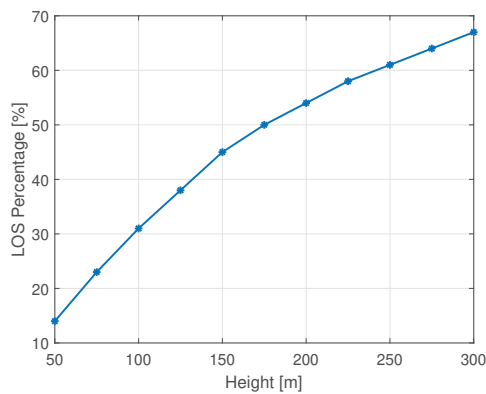


Fig. 2. Percentage of terrestrial users in LOS with UAV at different heights.

with the UAV at different UAV heights. It is clear that in Air-to-Ground (A2G) communication, the height of the UAV has an impact on the LOS condition and the propagation environment between the terrestrial UE and UAV. Fig. 2 shows the percentage of the users in LOS with UAV. It can be seen that the number of users admitting LOS increases with the height of the aerial communication platform. If UAV is at 50m height, there are only 14% users in LOS, but when UAV is at 200m height the percentage increases to 54%, and the growth of LOS connections continues with the increasing height of the UAV. Since several countries have restrictions on flying the drones above 250m height, we have limited our focus on the UAV heights up to 250m.

Fig. 3 shows the Cumulative Distribution Function (CDF) of the user received power at five different UAV heights. Although we have considered multiple frequencies and UAV heights, for the better visualization of results the Fig. 3 represents only the CDF of received power at 3.5 GHz. It can be seen from Fig. 3 that at 50m altitude around 2% of the users were in outage as no signal path was found by ray tracing simulations with given number of reflections and diffraction. We note that according to Fig. 2 a large portion of users are in NLOS condition if UAV operates at 50m height from the ground. Therefore, compared to higher UAV altitudes, there is a large number of users suffering from low received powers as only diffracted paths exist between the user and the UAV. Fortunately, at 3.5 GHz, the received power levels with UAV at 50m height are still acceptable even for NLOS users, and hence we don't observe any outage due to minimum received power requirement which is generally -120 dBm. However, at higher carrier frequencies these CDF curves will be shift in the left direction, and the outage probability increases. In order to analyze the impact of drone height at different frequencies the results of mean received power level are shown in Fig. 4.

Fig. 4 shows a surface plot of the mean received power, where the x-axis and y-axis represent the frequency and height of the UAV in GHz and meters, respectively. The color bar shows the strength of the mean received power in dBm. It is important to recall that, as it can be seen in Fig. 3,

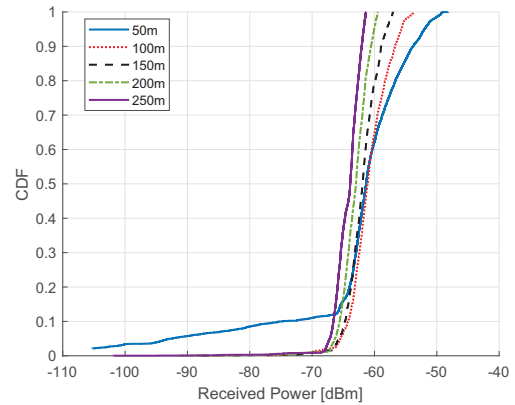


Fig. 3. CDF of received power at 3.5 GHz frequency with RT simulations.

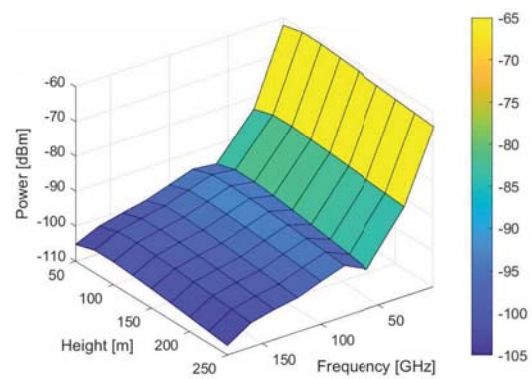


Fig. 4. Mean received power at different frequencies and drone heights with ray tracing simulations.

for low flying UAV, i.e. at 50m, the distance between the terrestrial user and the UAV is low. Therefore, there are users with very high received power. However, at the same time there is also a large number of users at cell border/edge. Whereas, with the increase in UAV height from 50m to 75m, although the distance between the terrestrial user and the UAV is increased, the additional height also improves the LOS probability between the UAV and the user, and increased height improves the coverage within the cell. This fact can be observed in Fig. 4 as mean received power level with 75m UAV altitude is better than with the 50m altitude but also better than in cases where UAV is at higher altitudes. In other words, for a given scenario and user grid, the UAV altitude of 75m is found as an optimal height in terms of received power. Fig. 4 also shows a sharp change in the received power level as the mean received power level drops by almost 20.5 dB and 33.5 dB while migrating from 3.5 GHz to 28 GHz and 60 GHz, respectively. Actually, due to significantly high atmospheric absorption at 60 GHz compared to 80 GHz, despite of higher frequency of operation the mean received power is found slightly better at 80 GHz compared to 60 GHz. After 80 GHz a gradual drop in mean received power level is witnessed up to 180 GHz. The lowest mean received power of -107 dBm is found with 180 GHz at 250m height. We recall that in our

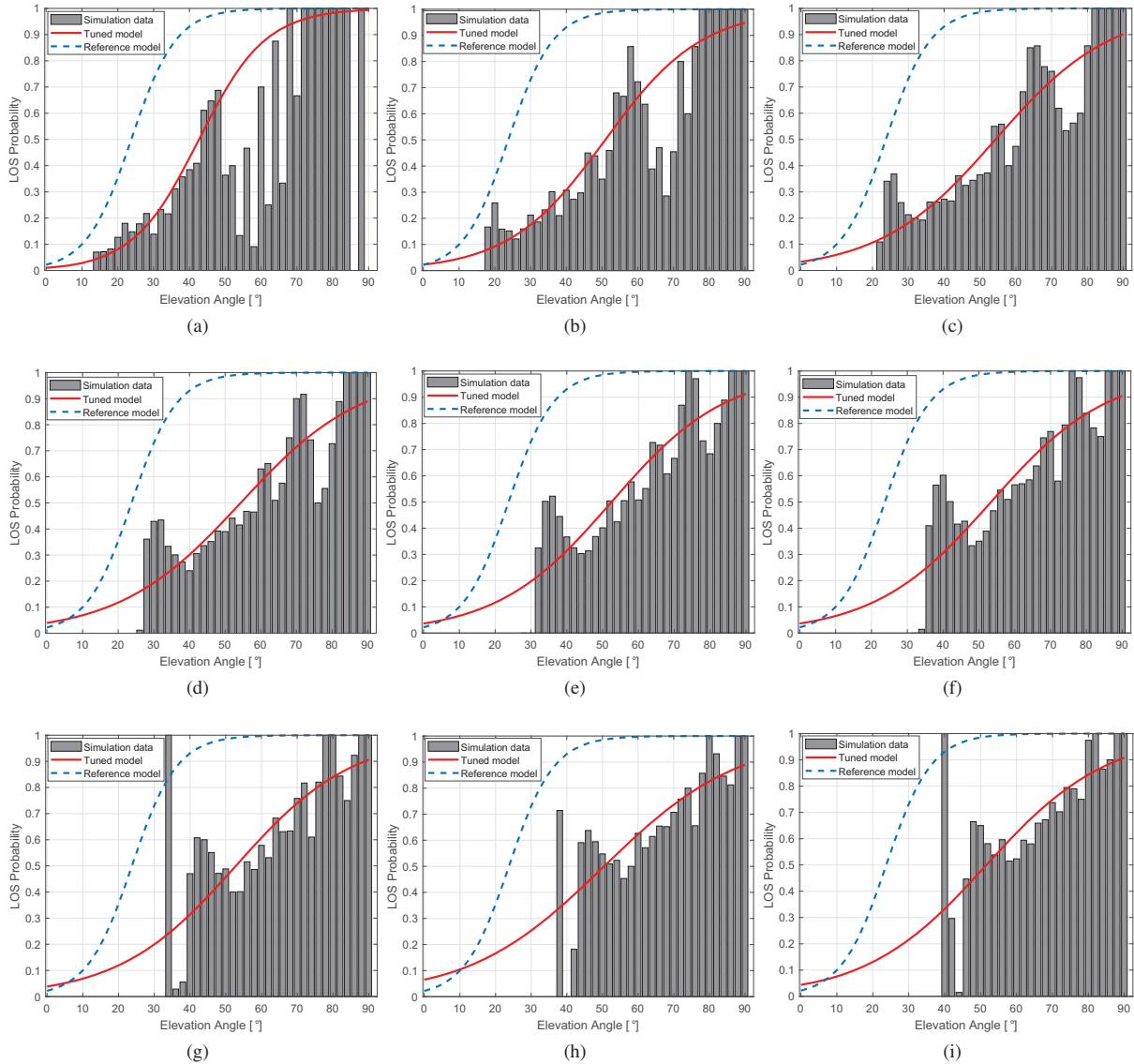


Fig. 5. LOS probability acquired through ray tracing simulation data and through LOS probability models at, (a) 50 m, (b) 75 m, (c) 100 m, (d) 125 m, (e) 150 m, (f) 175 m, (g) 200 m, (h) 225 m, and (i) 250 m UAV height..

simulations we have not considered any antenna gain at the transmitter and receiver side.

Fig.5(a-i) show the LOS probability against the elevation angle in degrees for the ray tracing simulation data at different heights of the UAV. The same uniform user distribution as shown in Fig.1(b) is used. In addition to simulated results, Fig.5 also shows the LOS probability obtained from the reference model and the tuned LOS probability model. We recall that the tuned LOS probability model is obtained by adjusting parameters  $a$  and  $b$  in Eq. 1 based on the acquired ray tracing simulation data. The values of parameters  $a$  and  $b$  used in tuned model are shown in Fig. 6 for different UAV heights, whereas the reference model assumes  $a = 9.61$  and  $b = 0.16$ . The simulation data in Fig.5 shows that the elevation angle has a wide spread at low UAV altitudes, and the spread of the

elevation angle decreases with the increase in the height of the UAV. This is expected results due to limited cell area. Also, at large elevation angles i.e. above  $75^\circ$  the UAV is almost on top of the user and accordingly the LOS probability is high. Interestingly, there is a significant difference between the reference model and the tuned model. The reference model is found clearly over optimistic as the LOS probability given by the reference model is quite high in comparison with the actual simulation data. Therefore, our simulation based values for  $a$  and  $b$  provide more realistic results.

Fig 7(a) and Fig 7(b) show the CDFs of LOS probability for different UAV heights which are found by using reference LOS probability model and our proposed tuned LOS probability model, respectively, for a given user distribution in Fig.1(b). There is a huge difference between the LOS probability results

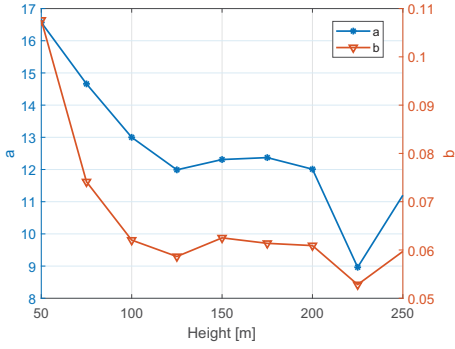
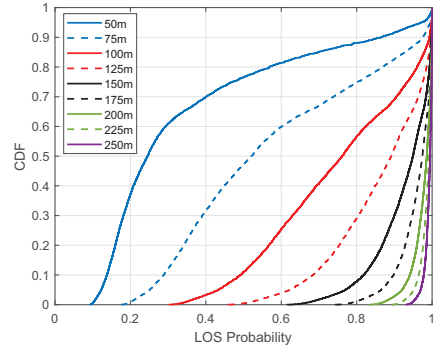


Fig. 6. Tuned values of parameter 'a' and 'b' with respect to ray tracing data.

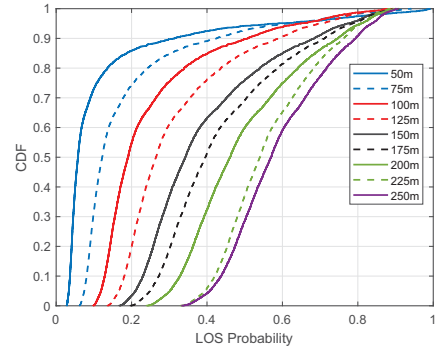
acquired through these two models. It is critical to highlight here that the parameters of the reference LOS probability model given in the paper [11] was for low altitude platforms which fly at an altitude of upto few thousand meters, Whereas, in the study of this paper we are mainly targeting really low flying drones starting from 50m altitude to a maximum height of 250m. Here, it is interesting to analyze the 10<sup>th</sup> percentile and 50<sup>th</sup> percentile values of the LOS probability curves. For example, the 10<sup>th</sup> value of LOS probability CDF with reference model is 0.82, 0.94, and 0.98, whereas with tuned model it is 0.23, 0.33, and 0.44 for 150m, 200m, and 250m, respectively. The 50<sup>th</sup> percentile score with reference model is almost close to 1 for UAV height above 150m, whereas on the other hand the 50<sup>th</sup> percentile score is significantly low with our tuned model as compared to reference model. The behavior of reference model becomes close to identical above 175m, and clearly seems over optimistic as the LOS probability is exigitly high. Whereas, the tuned model is giving realistic results and shows a fair approximate of LOS probability in a real world scenario. Similarly, other statistical comparisons can be directly made for other UAV heights and at different percentile score levels from the results presented in the Fig 7.

One of the variable in Eq 3 is  $\eta_{NLOS}$ , and that is the average additional NLOS loss given in dB. We have considered four different values of  $\eta_{NLOS}$  i.e. 5, 10, 15 and 20 dB, and Fig 8(a) and Fig 8(b) show the selected value of  $\eta_{NLOS}$  parameter that gives the minimum RMSE for reference and tuned LOS probability model, respectively. In Fig 8(a), for reference model the surface plot is mainly dominated by  $\eta_{NLOS} = 20dB$  except at 3.5 GHz. Whereas, in Fig 8(b) for tuned model there is a clear pattern showing that at 3.5 GHz and 28 GHz the recommended value for  $\eta_{NLOS}$  is 5 dB, at 60 GHz it is 15 dB, and at 80 GHz and above frequencies the minimum RMSE is achieved with  $\eta_{NLOS}$  equals to 10 dB. This way, we have found the link of  $\eta_{NLOS}$  with UAV height and frequency of operation.

Finally, Fig 9 shows three-dimensional plot of RMSE of received power between RT and other propagation models. In both Fig 9(a) and Fig 9(b), the worst RMSE is reported for low UAV height i.e., 50m altitude. The acquired RMSE is quite high i.e. around 8-8.5dB at 50m UAV height, and that is mainly due to the presence of far serving NLOS users.



(a)



(b)

Fig. 7. CDF of LOS probability, (a) Reference LOS probability model, and (b) Tuned LOS probability model.

Similarly, at 75m height the RMSE is upto 6 dB with reference model, whereas the maximum RMSE at 75m UAV height is limited to 4.5 dB with our proposed tuned model. However, the real gain of our proposed model over reference model is found at altitudes above or equals to 100m. Tuned model outperforms the reference model and shows a significant improvement in RMSE, as clearly evident by comparing Fig 9(a) and Fig 9(b).

## V. CONCLUSION

The radio propagation characteristics of UAV communication was studied using real building data from downtown Helsinki and 3D ray tracing simulations. Our focus was in line-of-sight (LOS) probability that is an important factor especially in mmWave communication. Results include the percentage of terrestrial UEs in LOS with UAV and received power levels obtained at different carrier frequencies and UAV heights. In addition to 3D ray tracing simulations we recall a previously published analytical model for LOS and redefine its parameters for different UAV heights.

As expected, the percentage of locations in LOS increases with the UAV height. Ray tracing simulation results revealed that at 50m UAV height the LOS percentage was 14% and it grew up to 68% when reaching the 300m height. The ray tracing simulation data also indicates that the LOS probability function with the parameters given in the reference paper [14] gives highly optimistic and unrealistic LOS probability compared with the ray tracing data. Accordingly, we proposed a

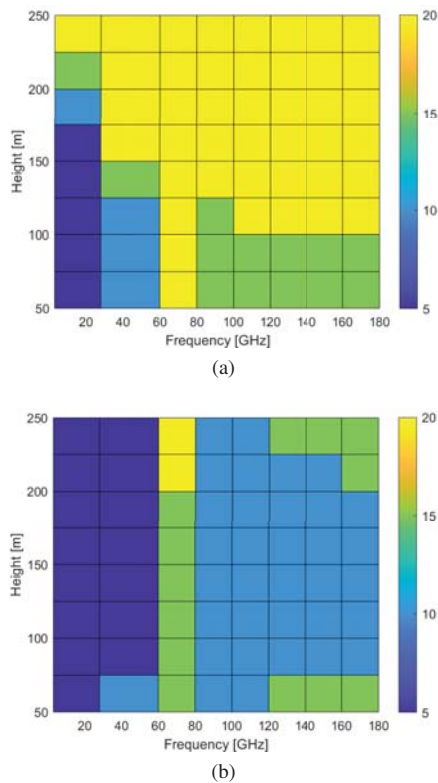


Fig. 8. Selection of NLOS loss parameter for minimum RMSE, (a) Reference LOS probability model, and (b) Tuned LOS probability model.

new set of parameters which are acquired by using curve fitting based on ray tracing results. Furthermore, a recommended value for the NLOS loss parameter in the analytical pathloss model was also given for different operation frequencies and UAV heights. The set of parameters given in this paper helps in reducing the RMSE between the ray tracing simulation results and analytical results.

#### ACKNOWLEDGEMENT

This research has been partially supported by the PriMO-5G and TERAWAY projects funded by the European Unions Horizon 2020 research and innovation programme under grant agreement No 815191 and No 871668, respectively.

#### REFERENCES

- [1] M. U. Sheikh, J. Säe, and J. Lempiäinen, "In preparation towards future cellular networks: the detailed analysis of macro and micro site densification and sector densification," *Telecommunication Systems*, vol. 65, no. 4, pp. 621–636, Aug 2017.
- [2] A. Al-Hourani, S. Kandeepan, and A. Jamalipour, "Modeling air-to-ground path loss for low altitude platforms in urban environments," in *2014 IEEE Global Communications Conference*, 2014, pp. 2898–2904.
- [3] A. Fotouhi, M. Ding, and M. Hassan, "Dronecells: Improving 5g spectral efficiency using drone-mounted flying base stations," *CoRR*, vol. abs/1707.02041, 2017. [Online]. Available: <http://arxiv.org/abs/1707.02041>
- [4] —, "Flying drone base stations for macro hotspots," *IEEE Access*, vol. 6, pp. 19 530–19 539, 2018.
- [5] M. Mozaffari, W. Saad, M. Bennis, Y.-H. Nam, and M. Debbah, "A tutorial on uavs for wireless networks: Applications, challenges, and open problems," *IEEE communications surveys & tutorials*, vol. 21, no. 3, pp. 2334–2360, 2019.

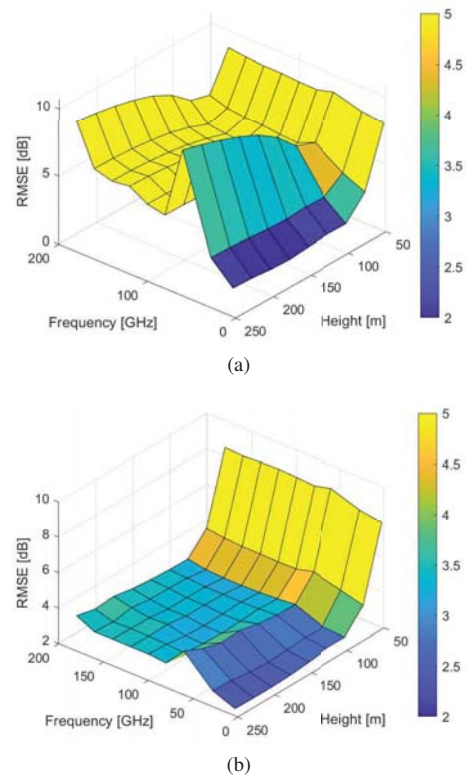


Fig. 9. Root mean square error between ray tracing and, (a) Reference LOS probability model, (b) Tuned LOS probability model.

- [6] T. Nagatsuma, "Advances in terahertz communications accelerated by photonics technologies," in *2019 24th OptoElectronics and Communications Conference (OECC) and 2019 International Conference on Photonics in Switching and Computing (PSC)*, 2019, pp. 1–3.
- [7] T. S. Rappaport, J. N. Murdock, and F. Gutierrez, "State of the art in 60-ghz integrated circuits and systems for wireless communications," *Proceedings of the IEEE*, vol. 99, no. 8, pp. 1390–1436, 2011.
- [8] M. Lecci, P. Testolina, M. Giordani, M. Polese, T. Ropitault, C. Gentile, N. Varshney, A. Bodi, and M. Zorzi, "Simplified ray tracing for the millimeter wave channel: A performance evaluation," *ArXiv*, vol. abs/2002.09179, 2020.
- [9] S. Soni and A. Bhattacharya, "An Efficient Two-Dimensional Ray-Tracing Algorithm For Modeling of Urban Microcellular Environments," *International Journal of Electronics and Communications*, vol. 66, no. 6, pp. 439 – 447, June. 2012.
- [10] M. U. Sheikh, F. Ghavimi, K. Ruttik, and R. Jantti, "Drone detection and classification using cellular network: A machine learning approach," in *2019 IEEE 90th Vehicular Technology Conference (VTC2019-Fall)*, 2019, pp. 1–6.
- [11] A. Al-Hourani, S. Kandeepan, and S. Lardner, "Optimal lap altitude for maximum coverage," *IEEE Wireless Communications Letters*, vol. 3, no. 6, pp. 569–572, 2014.
- [12] R. I. Bor-Yaliniz, A. El-Keyi, and H. Yanikomeroglu, "Efficient 3-d placement of an aerial base station in next generation cellular networks," in *2016 IEEE International Conference on Communications (ICC)*, 2016, pp. 1–5.
- [13] D. G. Cileo, N. Sharma, and M. Magarini, "Coverage, capacity and interference analysis for an aerial base station in different environments," in *2017 International Symposium on Wireless Communication Systems (ISWCS)*, 2017, pp. 281–286.
- [14] E. Kalantari, H. Yanikomeroglu, and A. Yongacoglu, "On the number and 3d placement of drone base stations in wireless cellular networks," in *2016 IEEE 84th Vehicular Technology Conference (VTC-Fall)*. IEEE, 2016, pp. 1–6.